
Article:
Frydrych, M. and Chen, B. (2017) Fabrication, structure and properties of three-dimensional biodegradable poly(glycerol sebacate urethane) scaffolds. Polymer , 122. pp. 159-168. ISSN: 0032-3861

https://doi.org/10.1016/j.polymer.2017.06.064

Fabrication, structure and properties of three-dimensional biodegradable poly(glycerol sebacate urethane) scaffolds

Martin Frydrych and Biqiong Chen*

Department of Materials Science and Engineering, University of Sheffield, Mappin Street, Sheffield, S1 3JD, United Kingdom.

*To whom correspondence should be addressed.

Fax: +44 (0) 114 222 5943

Tel: +44 (0) 114 222 5958

E-Mail: biqiong.chen@sheffield.ac.uk

Abstract

Large, three-dimensional, porous poly(glycerol sebacate urethane) (PGSU) scaffolds were fabricated via a solvent-based synthesis approach followed by freeze-drying and curing. The scaffolds showed highly interconnected open-cell structures with porosities and pore sizes in the ranges of 77-88% and 55-74 μm, respectively. The mechanical properties were measured in dry and hydrated states during quasi-static and cyclic tensile and compression tests. Hydrated PGSU scaffolds featured tensile Young moduli, ultimate tensile strengths and elongations at break in the ranges of 29-32 kPa, 12-19 kPa and 50-57%, respectively. *In vitro* degradation tests of the PGSU scaffolds presented adjustable degradation rates and mass losses of 10-16% and 30-62% without and with the presence of lipase enzyme in 112 days, respectively. This work illustrates that the large and porous PGSU scaffolds, characterised with flexible and soft mechanical properties, as well as long-term stability and adjustable degradation kinetics, have high potential for applications in soft tissue engineering.

Keywords: Bioelastomer, tissue scaffold, mechanical properties, soft tissue engineering.

1 Introduction

The development of synthetic and biodegradable scaffolds that mimic the structures and mechanical properties of native tissues are crucial objectives in the approach of regenerative medicine-based treatments.[1,2] In soft tissue engineering, synthetic biodegradable elastomers are a new emerging class of scaffold materials, capable of matching the host tissues structurally and mechanically.[3] Poly(glycerol sebacate) (PGS) is a biocompatible and biodegradable elastomer, specifically designed for soft tissue applications.[4] It is a covalently crosslinked polyester with tuneable and stretchable properties, characterised with a three-dimensional (3D) network which is capable of sustaining and recovering from deformations in mechanically dynamic environments.[4,5] Depending on the synthesis conditions, PGS presented tensile Young's moduli, strengths and strains at break in the ranges of 0.05-2.12 MPa, 0.23-0.79 MPa and 69-448%, respectively.[4–7] The *in vivo* degradation properties of PGS are characterised by surface erosion, relatively linear degradation kinetics and good retention of mechanical strength, with complete *in vivo* degradation within 60 days.[4,5,7] Despite encouraging results, processing of pristine PGS into large and 3D interconnected porous scaffold structures still remains challenging.[5,6] The harsh curing conditions of PGS, designated by high curing temperatures of 110-165 °C and long curing times of 12-114 h in vacuum environment, are limiting its fabrication feasibility.[5–7] Recently we developed large and highly porous PGS/poly(L-lactic acid) (PLLA) blend scaffolds for soft tissue applications *via* a freeze-drying and a subsequent curing process.[6,8] PLLA acted in this fabrication strategy as a structure-supporting polymer due to its high melting point, helping maintain a porous scaffold structure during the harsh curing conditions of PGS.[6,8] However, the porous PGS/PLLA blend scaffolds were still characterised with fast degradation kinetics, which could potentially be too fast to support the growth of certain target tissues or organs.[6,8] With this respect, the use of PGS in a broader spectrum of soft tissue engineering applications is

still limited, due to its relatively narrow adjustable mechanical range and fast degradation rates.[9]

Poly(glycerol sebacate urethane) (PGSU) was recently designed to overcome these limitations.[9] PGSU is a biocompatible and highly tuneable elastomer, synthesised by reacting PGS pre-polymer with an isocyanate-based crosslinker, such as hexamethylene diisocyanate (HDI). It can be synthesised rapidly under mild conditions through a solvent-based or solvent-free method, avoiding the time-consuming and harsh curing conditions of pristine PGS.[9,10] The mechanical and biodegradation properties of PGSU can be readily tailored by varying the synthesis method and the content of the crosslinker.[9,10] PGSU featured broad mechanical properties with Young's moduli, strengths and strains at break in the ranges of 0.7-19.7 MPa, 1.0-12.1 MPa and 78-516%, respectively.[9,10] The biodegradation of PGSU is dominated by surface erosion and presented *in vivo* degradation rates of over 40 weeks.[9] PGSU specimens presented no significant signs of inflammatory responses *in vivo* and the presence of sol content had no effect on its biocompatibility profile.[9] Previous studies on PGSU and their nanocomposites were mainly focused on their chemical structures, physical properties and biocompatibility.[9,10] While the fabrication of thin PGSU scaffolds by using water as a chemical blowing agent showed promising results,[9] the fabrication and analysis of the structure and properties of large and 3D interconnected porous PGSU scaffolds were still lacking.

In this study, flexible and large 3D porous PGSU scaffolds with three different low contents of HDI were fabricated through a freeze-drying process. For the fabrication of PGSU scaffolds 1,4-dioxane was used as a solvent, which is commonly used for freeze-drying synthetic polymers.[6,8] The morphology of the PGSU scaffolds was analysed by scanning electron microscopy (SEM), the hydrophilic characteristics and water absorption of the scaffolds were evaluated, the mechanical properties were investigated in depth in dry and

hydrated states during quasi-static and cyclic tensile and compression tests, along with rheological measurements. *In vitro* degradation studies up to 112 days were performed in enzyme-free and enzyme-containing phosphate buffer saline (PBS) solutions. The chemical structure and physical characteristics of PGS pre-polymer (pre-PGS) and PGSU films were also examined to assist our understanding of the PGSU scaffolds.

2 Materials and Methods

2.1 Materials

Sebacic acid, glycerol, HDI, Tin(II) 2-ethylhexanoate (Tin(II)), ethanol, 1,4-dioxane, dimethylformamide (DMF), acetone, dimethyl carbonate (DMC), toluene, chloroform, PBS tablets (for preparing a PBS-water solution of pH 7.4) and lipase enzyme from porcine pancreas (54 U mg^{-1}) were all of analytical grade and purchased from Sigma-Aldrich.

2.2 Preparation of PGS Pre-Polymer, PGSU Films and Scaffolds

PGS pre-polymer (pre-PGS) was synthesised according to previously reported methods, in which a molar ratio of 1:1 of sebacic acid and glycerol was reacted at 120 °C for 72 h under nitrogen gas and continuous stirring.[4,11]

Table 1. Material compositions of the PGSU solutions for freeze-drying.

Sample code	Molar ratio of glycerol to HDI / mol:mol	Mass ratio of Pre-PGS to HDI / g:g	Solvent	Solvent quantity / mL
PGSU-1:0.4	1:0.4	1.42:0.33	1.4-dioxane	50
PGSU-1:0.5	1:0.5	1.36:0.39	1.4-dioxane	50
PGSU-1:0.6	1:0.6	1.30:0.45	1.4-dioxane	50

PGSU specimens with three different molar ratios of glycerol to HDI (glycerol:HDI = 1:0.4; 1:0.5, 1:0.6) were synthesised on the basis of a prior solvent-based method.[9] These low

molar ratios of glycerol to HDI were chosen to guarantee soft and flexible properties.[9] The nomenclature of the synthesised specimens is presented as PGSU-X, where "X" represents the molar ratio of glycerol to HDI: PGSU-1:0.4, PGSU-1:0.5 and PGSU-1:0.6. Briefly, pre-PGS was dissolved in 1.4-dioxane under the presence of the catalyst Tin(II) (0.05% w/v) and heated to 55 °C under constant stirring in a sealed flask. HDI was then added drop wise to the solution, with nitrogen purged into the reaction flask which was sealed and held at 55 °C for 5 h. For the preparation of PGSU films, the solution was cast onto a Teflon dish and left for 2 days in a fume cupboard at room temperature, and then kept for 2 days in a vacuum oven at 37 °C to evaporate any residual solvent and allow for further crosslinking.[9,10] For the preparation of PGSU scaffolds, the solutions were cast into a non-sticky Teflon-coated metal tray (six cylindrical cavities; diameter = 60 mm; purchased from a local store) and placed in a freeze-dryer (FreeZone Triad Freeze Dry System, Labconco Co.) for lyophilisation. With this respect, the PGSU scaffolds were prepared with a fixed total material concentration, as listed in Table 1, and fabricated via a modified freeze-drying procedure, based on our previous methods.[6,8] Briefly, the solutions were cooled to -30 °C and held for 5 h. The frozen solutions were heated to -5 °C (heating rate of 1 °C min^{-1}) and sublimated for 24 h under vacuum. The temperature was raised to room temperature (cooling rate of 1 °C min^{-1}) and held for 5 h, completing the freeze-drying procedure. The as-prepared specimens were left for 2 days in a fume cupboard at room temperature, and then kept for 2 days in a vacuum oven at 37 °C to evaporate any residual solvent and to cure the specimens further.[9,10] All PGSU films and scaffolds underwent a cleaning procedure prior to tests (24 h saturation in ethanol at 21 °C; vacuum oven drying at 37 °C for 24 h) and were stored in a standard 50% relative humidity at 21 °C until further use.

2.3 Characterisation of PGS Pre-polymer and PGSU Films

The number average molecular weight ($\overline{M}_n$), the weight average molecular weight ($\overline{M}_w$), and the polydispersity index (*PDI*) of the pre-PGS were obtained by gel permeation chromatography (GPC) as previously described.[8] Attenuated Total Reflectance Fourier Transform Infrared Spectroscopy (FTIR) was performed on a Perkin Elmer Spectrum One NTS analyser and the mid-infrared region of 4000-450 cm^{-1} with a resolution of 1 cm^{-1} recorded.

The solubility of PGSU film specimens was evaluated by 24 h solvent saturation in dimethylformamide, 1.4-dioxane, acetone, dimethyl carbonate, toluene, chloroform and ethanol at 21 °C. The sol content of non-cleaned PGSU film specimens (n = 5) was measured by determining the mass difference before and after 24 h ethanol saturation at 21 °C. The swelling properties of the dried PGSU specimens (n = 9) were analysed in PBS solution (pH = 7.4, 24 h saturation at 37 °C) and ethanol (24 h saturation at 21 °C), in which the mass swelling ratio was determined by dividing the mass gained during the fluid saturation by the mass of the initial sample.

The solid densities (ρ_s) of dry PGSU film specimens were obtained by using a helium pycnometer (AccuPycII 1340, Micromeritics) on pre-dried specimens. Quasi-static uniaxial tensile tests were performed on dry and hydrated (after 24 h saturation in the PBS solution at 37 °C) PGSU film specimens at ambient condition (21 °C). Punched-out PGSU film specimens (n = 5; “dog-bone” shaped; width: 2.6 mm, gauge length: 20 mm, thickness: 0.4 ± 0.05 mm) were tested on a Hounsfield H100KS testing machine (Tinius Olsen), using a strain rate of 50 mm min^{-1} and a 10 N load cell till fracture (ASTM D412).

2.4 Characterisation of PGSU Scaffolds

The microstructure analysis of as-prepared and cleaned PGSU scaffolds was performed by SEM (Camscan S2). The SEM observations were carried out at 5 kV on cubic samples from the centre of the scaffold cross section, which were beforehand gold-coated for 3 min at 15 mA by a sputter coater (Emscope SC500). The pore sizes (n = 450) of the scaffolds were analysed by using the image processing software ImageJ and only fully defined pores were used for measurements.

The scaffold densities were measured by weighing dry cubic specimens (n = 8) with an analytical balance (AB204-S, Mettler Toledo), while their volumes were measured by using a caliper. The relative density (ρ_r) and the porosity (P_f) of all scaffolds were calculated by Equation 1 and Equation 2 respectively,

$$\rho_r = \rho_f / \rho_s \quad (1)$$

$$P_f = (1 - \rho_r) \times 100\% \quad (2)$$

The water absorption behaviour within PGSU scaffolds (n = 9) was evaluated by calculating the mass difference between initial dry and soaked specimens, after 24 h saturation in PBS solution at 37 °C. The specimens were carefully wiped with filter paper to remove excess water on their surface, prior to mass measurements.

Quasi-static and cyclic tensile and compression tests were executed on dry and hydrated (after 24 h saturation in PBS solution at 37 °C) PGSU scaffold specimens at ambient condition (21 °C), by using a Hounsfield H100KS testing machine and a 10 N load cell. Stripe specimens were used for quasi-static (n = 10; width: 5.14 ± 0.70 mm, gauge length: 15 mm, thickness: 3.04 ± 0.71 mm) and cyclic (n = 3; width: 5.60 ± 0.78 mm, gauge length: 15 mm, thickness: 3.66 ± 0.82 mm) tensile tests, which were cut-out from the centre cross section of the scaffolds and tested in the longitudinal direction, according to a previously

established method.[6,8] Quasi-static uniaxial tensile tests were performed at a tensile strain rate of 50 mm min^{-1} till fracture (ASTM D412), while the cyclic tensile tests were stretched to 20% strain during 20 cycles, at the same tensile strain rate. Cylindrical samples used for quasi-static (n = 10; diameter: 10 mm, thickness: 4.13 ± 0.94 mm) and cyclic (n = 3; diameter: 10 mm, thickness: 5.99 ± 0.35 mm) compression tests were punched-out from the centre cross section of the scaffolds. Quasi-static uniaxial compression tests were performed at a strain rate of 5 mm min^{-1} up to a strain of 75%, while cyclic compression tests were compressed to 50% strain during 20 cycles, at the same strain rate.

Rheological measurements on hydrated (after 24 h saturation in PBS solution at 37 °C) PGSU scaffold specimens were executed on an Anton Paar Physica MCR 301 rheometer. Dynamic frequency sweep measurements were performed at 25 °C, over a frequency range of 0.1 to 10 Hz under a fixed strain of 0.1% (in the linear viscoelastic region; pre-determined by dynamic strain sweep tests), by using a fixed gap of 1 mm between two parallel plates (diameter: 12 mm). Punched-out cylindrical samples (diameter: 12 mm, thickness: 1 mm) from the centre cross section of the scaffolds were used.

In vitro degradation studies were performed on punched-out PGSU scaffold specimens (n = 3; diameter: 6 mm; thickness: 2.58 ± 0.12 mm) for up to 112 days at 37 °C, based on our prior work.[6,8] Briefly, tests were conducted in a shaker incubator (Stuart SI500; 100 rpm) with two separate degradation media: a lipase containing PBS solution (25 mL; enzyme concentration: 110 U L^{-1})[12] and a standard PBS solution (25 mL) as control. Both degradation media were changed every day, while the specimens were removed from the degradation media after specific days of incubation, washed with distilled water, dried in a vacuum oven at 37 °C, and weighed. SEM analysis was performed at 5 kV on gold coated PGSU scaffold specimens after 34 days' *in vitro* degradation.

2.6 Statistics

All measurements were reported as mean ± standard deviation (SD) with a confidence level of 95%. Differences were statistically tested against a null hypothesis of no difference between samples using a two sample t-test with equal variance not assumed (significance = $p < 0.05$).

3 Results and Discussion

3.1 Characterisation of PGS Pre-polymer and PGSU Films

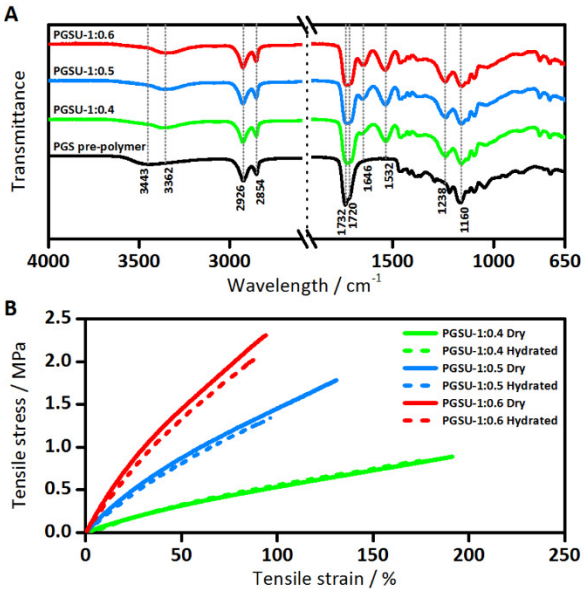

Figure 1. (A) FTIR spectra of pre-PGS and PGSU derivatives in the ranges of 4000-1000 cm^{-1}, respectively. The spectra were shifted vertically for clarity. (B) Representative quasi-static tensile stress-strain curves of dry and hydrated PGSU films.

The pre-PGS utilised for the solvent-based PGSU synthesis was characterised by GPC with a $\bar{M}_n$, $\bar{M}_w$ and *PDI* of 1550 g mol^{-1}, 10520 g mol^{-1} and 6.8, respectively. As seen in Figure 1 (A), the FTIR spectrum of pre-PGS shows the stretching vibration of -OH at 3443 cm^{-1}, C-H at 2926 cm^{-1} and 2854 cm^{-1}, C=O and C-O at 1732 cm^{-1} and 1160 cm^{-1}, respectively.[5,13,14]. In comparison, the PGSUs were characterised with the stretching vibration

of -OH and -NH at 3362 cm^{-1}, C-H at 2926 cm^{-1} and 2854 cm^{-1}, C=O and C-O at 1720 cm^{-1}, the bending vibration of amide I, II and III at 1646 cm^{-1}, 1532 cm^{-1} and 1238 cm^{-1}, and stretching vibration of C=O and C-O at 1160 cm^{-1}, respectively.[9,10] The amide groups are attributed to the formation of urethane, the reaction product of HDI and hydroxyl groups.[9,10] The crosslinking of pre-PGS and HDI resulted in peak shifts to lower wavenumbers (e.g. 3362 cm^{-1} and 1720 cm^{-1}), also indicating the establishment of urethane linkages and an increase in hydrogen bonding strength.[9,10] In addition, the PGSU elastomers with higher molar ratios of glycerol to HDI presented stronger amide-based absorption peaks, demonstrating a higher degree of urethane groups. The results confirm the successful formation of urethane linkages between pre-PGS and HDI to form PGSU, as previously reported.[9,10] The characteristic isocyanate group band at 2270 cm^{-1} was absent in all the PGSUs, implying the complete reaction of the groups.[9,10]

Table 2: Quasi-static tensile properties of dry and hydrated PGSU films (n = 5).

	Sample code	Young's modulus, E_s / MPa	Ultimate tensile strength, σ_{smax} / MPa	Elongation at break, ε_{sb} / %
Cleaned / dry	PGSU-1:0.4	0.84 ± 0.03	0.93 ± 0.07	199 ± 1.0
	PGSU-1:0.5	2.11 ± 0.11	1.55 ± 0.07	125 ± 18
	PGSU-1:0.6	3.98 ± 0.62	2.24 ± 0.45	91.6 ± 3.8
Cleaned / hydrated*	PGSU-1:0.4	0.84 ± 0.01	0.91 ± 0.04	186 ± 4.5
	PGSU-1:0.5	2.11 ± 0.03	1.44 ± 0.10	98.0 ± 4.1
	PGSU-1:0.6	3.51 ± 0.01	2.07 ± 0.12	90.8 ± 5.5

*24 h saturation in PBS at 37 °C.

All of the PGSUs were insoluble in various organic solvents (ethanol, acetone, 1.4-dioxane, DMF, DMC, toluene, chloroform), confirming the formation of a covalently crosslinked network. They are, however, swellable in these solvents. For instance, PGSU-1:0.4, PGSU-1:0.5 and PGSU-1:0.6 specimens presented relatively high mass swelling ratios

in ethanol (after 24 h saturation at 21 °C) of 88.2 ± 5.6%, 67.9 ± 1.3%, 55.9 ± 5.7%, while these specimens presented only low mass swelling ratios in aqueous PBS solution (24 h saturation at 37 °C) of 4.91 ± 0.93%, 3.99 ± 0.79% and 2.68 ± 0.93%, respectively. The PGSU elastomers with higher molar ratios of glycerol to HDI showed in general lower degrees of mass swelling ratios, which can be linked to a presumably higher crosslink density, while the overall low mass swelling ratios in PBS solution can be attributed to the primarily hydrophobic nature of the elastomer.[9] In respect to the residual analysis of non-cleaned PGSU-1:0.4, PGSU-1:0.5 and PGSU-1:0.6 specimens (after 24 h ethanol extraction), mass losses of 15.9 ± 2.0%, 5.4 ± 0.9% and 2.0 ± 1.0% were measured, indicating the existence of unreacted monomers, oligomers, and pre-polymers.[10] The PGSU specimens had a similar ρ_s of 1.164 ± 0.004 Mg m^{-3} to the value previously reported (1.15 Mg m^{-3}).[10]

As shown in Figure 1 (B), all the PGSUs were characterised with soft and highly flexible properties, which can be ascribed to the urethane crosslinks.[3,9,15] The tensile Young's modulus (E_s), the ultimate tensile strength (σ_{smax}) and the strain at break (ε_{sb}) were obtained for dry and hydrated PGSUs, as listed in Table 2. The tensile testing results of the cleaned and dry PGSUs demonstrated significant difference in terms of E_s, σ_{smax} and ε_{sb}. The mechanical properties of the cleaned and hydrated PGSUs also presented difference among themselves, with only one exception (the ε_{sb} results of the hydrated PGSU-1:0.5 and PGSU-1:0.6 specimens exhibited no statistical difference). So, in general the alteration of the HDI crosslinker ratio changed the mechanical characteristics of PGSU significantly. The dry and hydrated PGSU-1:0.4 specimens presented the softest and most flexible properties with E_s, σ_{smax} and ε_{sb} values of 0.84 MPa, 0.91-0.93 MPa and 186-199%, while the PGSU-1:0.5 and PGSU-1:0.6 specimens exhibited stiffer mechanical characteristics with E_s, σ_{smax} and ε_{sb} values in the ranges of 2.11-3.98 MPa, 1.44-2.24 MPa and 98-125%, respectively. The direct comparison of dry and hydrated PGSU counterparts demonstrated similar results, due to their

hydrophobicity as previously stated. Still, the hydrated PGSU specimens presented the tendency of decreased σ_{smax} and ε_{sb} results compared to their dry equivalents. It is assumed that the absorbed water molecules may interfere with the hydrogen bonding of urethane N-H groups and urethane or ester C=O groups, which affects the mechanical performance of polyurethanes.[3,15,16]

The crosslink density (n_{mech}) of dry PGSU film specimens were calculated based on the theory of rubber elasticity, given by Equation 3,[4]

$$n_{mech} = E_s/3RT \quad (3)$$

where R the universal gas constant, and T the absolute temperature during the tensile tests. All the PGSUs presented statistically significant difference in n_{mech}, which were calculated for PGSU-1:0.4, PGSU-1:0.5 and PGSU-1:0.6 as 113 ± 7 mol m^{-3}, 286 ± 15 mol m^{-3} and 539 ± 84 mol m^{-3}, respectively. The n_{mech} results correlate with the FTIR and swelling results discussed earlier. With this respect, previous studies demonstrated that minor differences in the molar ratio of HDI had substantial effects on the physicochemical properties of PGSU.[9]

3.2 Microstructures of PGSU scaffolds

PGSU scaffolds with three different molar ratios of HDI to glycerol and a fixed material concentration of 1.75 g per 50 ml were fabricated by freeze-drying. All as-prepared PGSU scaffolds were characterised by a white colour and dimensions of approximately 6 cm in diameter and over 1 cm in thickness, as demonstrated in Figure 2 (A1-3). These results demonstrate that the immediate freeze-drying of the PGSU pre-polymer/solvent polymerisation medium can lead to stable three-dimensional PGSU scaffold constructs. The surfaces of the PGSU samples revealed minor adhesive properties, due to the low crosslink density and/or the presence of unreacted oligomers or pre-polymer, indicating the necessity of additional cleaning procedures. As seen in Figure 2 (B1-3, C1-3), the execution of

cleaning procedures (24 h saturation in ethanol at 21 °C) on all the as-prepared PGSU scaffolds affected their physical shape and presented the tendency of specimen shrinkage, with the strongest effect on the PGSU-1:0.4 specimens. Thus, the scaffold microstructures of dry as-prepared and cleaned PGSU scaffolds were examined by SEM, analysing the impact of the cleaning procedure on the pore size and structure of the scaffold.

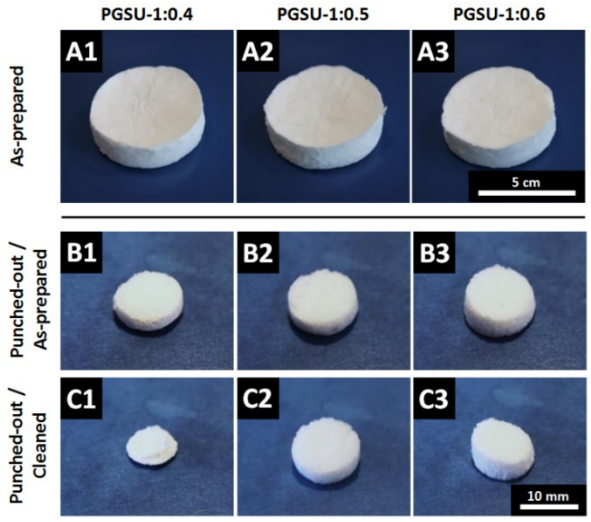

Figure 2. As-prepared scaffolds of (A1) PGSU-1:0.4, (A2) PGSU-1:0.5 and (A3) PGSU-1:0.6, directly after freeze-drying. Punched-out scaffold specimens of (B1, C1) PGSU-1:0.4, (B2, C2) PGSU-1:0.5 and (B3, C3) PGSU-1:0.6, before and after cleaning.

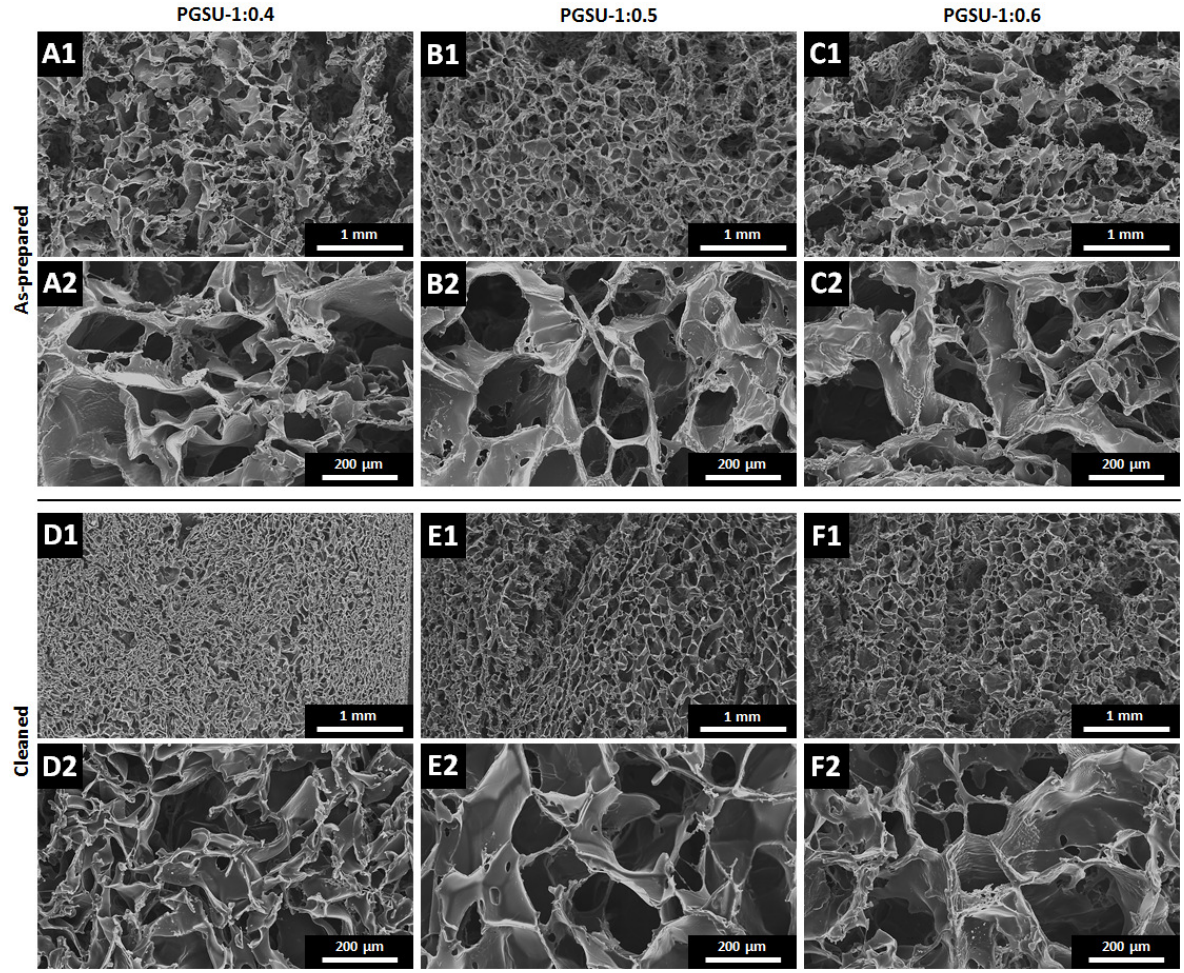

Figure 3. SEM micrographs of as-prepared (A1-2) PGSU-1:0.4, (B1-2) PGSU-1:0.5 and (C1-2) PGSU-1:0.6 scaffold microstructures, as well as cleaned (D1-2) PGSU-1:0.4, (E1-2) PGSU-1:0.5 and (F1-2) PGSU-1:0.6 scaffold microstructures.

All the as-prepared PGSU scaffolds showed randomly distributed and highly interconnected open-pore structures, illustrating relatively good distribution of the solid PGSU throughout the scaffold, as presented in Figure 3 (A1-2, B1-2, C1-2). The pores of the scaffold were characterised with non-uniform shapes, which are commonly found in freeze-dried PGS-based scaffolds with 1.4-dioxane as the solvent.[6,8] The as-prepared PGSU-1:0.4, PGSU-1:0.5 and PGSU-1:0.6 scaffolds featured broad pore size distributions (Figure S1, Supplementary Content), in which the PGSU-1:0.4, PGSU-1:0.5 and PGSU-1:0.6 scaffolds presented similar pore sizes of 93 ± 4 µm, 102 ± 3 µm and 112 ± 4 µm, respectively. The

variation of the HDI crosslinker ratio changes the average pore size of the PGSU scaffolds (at a fixed material concentration of the freeze-drying solution). Higher molar ratios of the HDI crosslinker lead to an increase in crosslink density, which improved the structural stability of the scaffold, due to more stable pore struts and walls in the microstructure.

As shown in Figure 3 (D1-2, E1-2, F1-2), all the cleaned PGSU scaffolds maintained a highly interconnected open-cell structure, but presented drops in pore size. The cleaned PGSU-1:0.4, PGSU-1:0.5 and PGSU-1:0.6 scaffolds featured a narrow pore size distribution and average pore sizes of 55 ± 1 µm, 74 ± 2 µm and 72 ± 4 µm, demonstrating a statistically significant pore size drop of 41.2%, 27.4% and 35.9%, compared to the as-prepared counter parts, respectively. The pore size drop resulted in more compact microstructures, in particular for the cleaned PGSU-1:0.4 scaffold specimens, as seen in Figure 3 (D1-2). The open-pore structure of the cleaned PGSU-1:0.4 scaffold specimens were characterised with less defined pore shapes and struts, while the cleaned PGSU-1:0.5 and PGSU-1:0.6 scaffolds featured larger and better preserved pore shapes. The overall drop in pore sizes can be linked to the cleaning procedure, owing to the self-loaded deformation of the ethanol swollen PGSU matrix, as well as due to the sol content removal. Thus, the self-supporting microstructures of the PGSU scaffolds collapsed due to the high mass swelling ratio in ethanol. The PGSU-1:0.5 and PGSU-1:0.6 specimens featured a higher crosslink density and were less swellable, contributing to greater scaffold structure stability. Previous studies also showed that cleaning or sterilization treatments affected the physical properties of polymer scaffolds, resulting in changed pore sizes and scaffold dimensions.[17–19] Nevertheless, the final pore structure (e.g. pore size and porosity, *vide infra*) of the PGSU scaffolds could be further optimised by altering the solution concentration and the freeze-drying parameters (e.g. the freezing temperature, the total freezing time, and the cooling rate),[6,8] demonstrating a high fabrication flexibility.

3.3 Physical and mechanical properties of PGSU scaffolds

Table 3. Densities and porosities of PGSU scaffolds (n = 8).

Sample code	Scaffold density, ρ_f / Mg m^{-3}	Relative density, $\rho_r = \rho_f / \rho_s$	Porosity, P_f / %
PGSU-1:0.4	0.265 ± 0.042	0.227 ± 0.036	77.3 ± 3.6
PGSU-1:0.5	0.170 ± 0.014	0.147 ± 0.012	85.3 ± 1.2
PGSU-1:0.6	0.141 ± 0.009	0.121 ± 0.007	87.9 ± 1.3

The cleaned PGSU-1:0.5 and PGSU-1:0.6 scaffolds were characterised with relatively high porosities in the range of 85-88%, while the PGSU-1:0.4 scaffolds featured a lower porosity of 77%, as listed in Table 3. Overall, the porosities of the PGSU scaffolds align with the pore sizes discussed previously.

Table 4. Quasi-static tensile and compression properties of dry and hydrated PGSU scaffolds (n = 10).

		Tensile			Compression	
	Sample code	Young's modulus, E_t / kPa	Ultimate tensile strength, σ_{tmax} / kPa	Elongation at σ_{tmax}, $\varepsilon_{t\sigma max}$ / %	Young's modulus, E_c / kPa	Comp. stress at $\varepsilon_{c75\%}$, $\sigma_{c75\%}$ / kPa
Cleaned / dry	PGSU-1:0.4	40 ± 3	18 ± 4	49 ± 4	20 ± 7	75 ± 19
	PGSU-1:0.5	38 ± 13	16 ± 4	55 ± 3	6 ± 1	39 ± 7
	PGSU-1:0.6	30 ± 1	22 ± 1	82 ± 9	5 ± 1	32 ± 4
Cleaned / hydrated*	PGSU-1:0.4	29 ± 14	16 ± 4	52 ± 5	8 ± 1	43 ± 10
	PGSU-1:0.5	32 ± 6	12 ± 3	50 ± 1	4 ± 1	29 ± 5
	PGSU-1:0.6	29 ± 3	19 ± 3	57 ± 2	3 ± 1	13 ± 1

*24 h saturation in PBS at 37 °C.

The water absorption abilities of the PGSU scaffolds were evaluated by immersing specimens for 24 h in PBS solution at 37 °C. The PGSU-1:0.5 and PGSU-1:0.6 scaffolds presented significant difference in the water swelling degree at equilibrium, compared to the PGSU-1:0.4 specimens. The PGSU-1:0.5 and PGSU-1:0.6 scaffolds obtained similar high water swelling ratios of 970 ± 127% and 1052 ± 72%, while the PGSU-1:0.4 specimens presented a lower value of 385 ± 25%. The results imply that the water absorption ability is

mainly dependent on the scaffold porosity or void volume.[20] The aqueous PBS solution was mainly absorbed in the pores of the scaffolds, in which higher scaffold porosities resulted into higher water absorption capabilities, and *vice versa*. In contrast, the low mass swelling ratios of the PGSU solid materials had a minor effect on the water absorption abilities of the porous scaffolds.

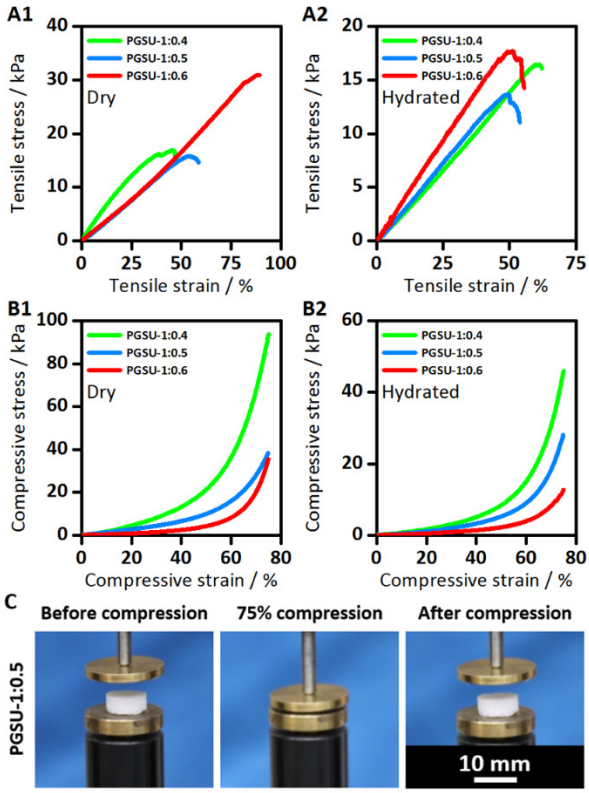

Figure 4. Representative quasi-static tensile stress-strain curves of (A1) dry and (A2) hydrated PGSU scaffolds. Representative quasi-static compressive stress-strain curves of (B1) dry and (B2) hydrated PGSU scaffolds. Compressive tests were terminated at a strain of 75%. (C) Compressive behaviour of dry PGSU scaffolds, illustrating the shape restorability after released compression load.

The mechanical properties of cleaned PGSU scaffolds were determined under dry and hydrated states by quasi-static and cyclic tensile and compression tests. Representative tensile stress-strain curves of the scaffolds are presented in Figure 4 (A1-2). The tensile Young's modulus (E_t), the ultimate tensile strength (σ_{tmax}) and the elongation at ultimate tensile

strength ($\varepsilon_{t\sigma max}$) were obtained, as listed in Table 4. The results showed that the PGSU scaffolds are highly flexible in dry and hydrated conditions; no yielding was observed in the testing curves before failure occurred. At cleaned and dry state, all the PGSU scaffolds presented similar E_t and σ_{tmax} results in the ranges of 30-40 kPa and 16-22 kPa, respectively, while the PGSU-1:0.6 scaffold exhibited with significant difference a high $\varepsilon_{t\sigma max}$ of 82% compared to the other two scaffolds. The physical characteristics of the PGSU-1:0.6 scaffold such as a large pore size and high porosity,[21] as well as the relatively high ductility of the solid PGSU promoted the overall good $\varepsilon_{t\sigma max}$ properties. At cleaned and hydrated state, all the PGSU scaffolds obtained also similar E_t and σ_{tmax} results. The hydrated PGSU-1:0.6 scaffold exhibited a low E_t of 29 kPa and the highest $\varepsilon_{t\sigma max}$ of 57%, representing a significant difference to the PGSU-1:0.5 scaffold. The comparison of the tensile properties between dry and hydrated counterparts demonstrated no significant difference for the PGSU-1:0.4 and PGSU-1:0.5 scaffolds; however, the hydrated PGSU-1:0.6 scaffold exhibited decreased σ_{tmax} and $\varepsilon_{t\sigma max}$ results of 14% and 30%, respectively, compared to its dry counterparts. The results indicate that the mechanical properties of the PGSU scaffolds may be affected under hydrated conditions, as the absorbed water molecules may influence the hydrogen-bonding interactions between urethane and ester linkages within the polymer network.[3,15,16]

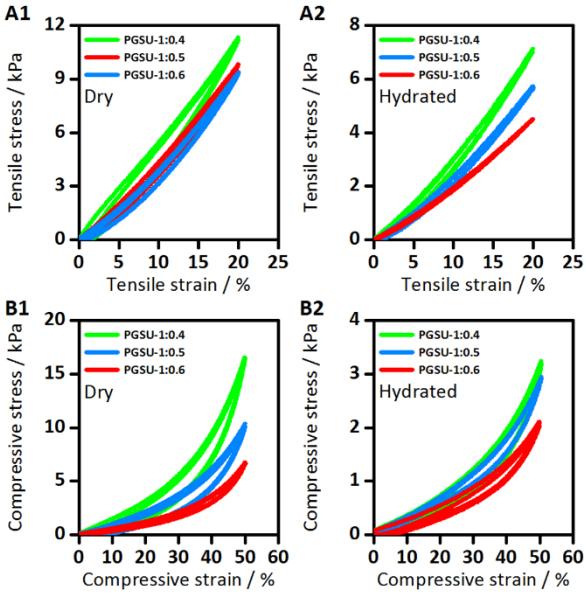

Figure 5. Representative cyclic tensile tress-strain curves of (A1) dry and (A2) hydrated PGSU scaffolds. Representative cyclic compressive stress-strain curves of (B1) dry and (B2) hydrated PGSU scaffolds.

Figure 4 (B1-2) shows representative compressive stress-strain curves of dry and hydrated PGSU scaffolds. For the compression tests the Young's modulus (E_c) and the compressive stress at 75% strain ($\sigma_{c75\%}$) were measured, as listed in Table 4. All the PGSU scaffolds were able to withstand the high compression and presented full shape recovery after the release of load, both in dry and hydrated state, as demonstrated in Figure 4 (C) (Figure S2, Supplementary Content). In addition, all the PGSU scaffolds were characterised with only a linear elastic and a densification regime, with no presence of a collapse plateau, indicating no structure collapse or fracture.[22] At cleaned and dry state, the PGSU-1:0.6 and PGSU-1:0.5 scaffolds showed similar E_c and $\sigma_{c75\%}$ results in the ranges of 5-6 kPa and 32-39 kPa, while the PGSU-1:0.4 scaffold featured significantly higher E_c and $\sigma_{c75\%}$ values of 20 kPa and 75 kPa, respectively. In this respect, the relatively dense microstructure of the PGSU-1:0.4 scaffold, characterised with small pore sizes and low porosity, resulted in stiffer scaffold constructs. At cleaned and hydrated state the hydrated PGSU-1:0.6 scaffold obtained the lowest E_c and $\sigma_{c75\%}$ of 3 kPa and 13 kPa, respectively. The comparison of the compressive

properties between dry and hydrated counterparts demonstrated the tendency of an E_c decrease under hydrated state; however, only the hydrated PGSU-1:0.4 scaffolds exhibited a significant decrease in E_c of 40%. Also, the hydrated PGSU-1:0.4 and PGSU-1:0.6 scaffolds exhibited significant decreases in $\sigma_{c75\%}$ of 43% and 59%, respectively. The results indicate the tendency that the E_c and $\sigma_{c75\%}$ values of dry and hydrated PGSU scaffolds are dependent on their porosities and pore sizes, and that the mechanical properties may be affected under hydrated conditions.

Cyclic tensile and compressive stress-strain curves of dry and hydrated PGSU scaffolds presented relatively minimal hysteresis loop during loading, as seen in Figure 5 (A1-2, B1-2). The hysteresis (e_d) was evaluated by defining a hysteresis loss ratio (h_r), expressed by Equation 4,[23]

$$h_r = \frac{e_0 - e_r}{e_0} = \frac{e_d}{e_0} \quad (4)$$

where e_0 and e_r are the input and retraction strain-energy densities of the loading and unloading curves, respectively. Under cyclic tensile testing, the dry PGSU-1:0.4, PGSU-1:0.5 and PGSU-1:0.6 scaffolds were characterised with a h_r of 0.17, 0.12 and 0.07, while hydrated PGSU-1:0.4, PGSU-1:0.5 and PGSU-1:0.6 scaffolds were characterised with a negligible low h_r of 0.07, 0.08 and 0.04 after 20 cycles of tensile loading to 20% strain, respectively. With respect to cyclic compressive testing, the dry PGSU-1:0.4, PGSU-1:0.5 and PGSU-1:0.6 scaffolds were characterised with a h_r of 0.29, 0.36 and 0.17, while the hydrated PGSU-1:0.4, PGSU-1:0.5 and PGSU-1:0.6 scaffolds were characterised with a decreased h_r of 0.20, 0.14 and 0.19 after 20 cycles of compressive loading to 50% strain, respectively. It is assumed that the expelling of water during the performed cyclic compressive tests resulted in higher h_r results.[24] Nevertheless, all PGSU scaffolds were fully recoverable after cessation of the cyclic tensile and compression loadings under dry and

hydrated state. The PGSU-1:0.6 scaffold presented overall best resilience characteristics, due to the low h_r values under dry and hydrated states. The low hysteresis properties can be attributed to the higher crosslink density within the generally lightly crosslinked PGSU scaffolds, which improved the load transfer efficiency of the polymer networks under dry and hydrated conditions.

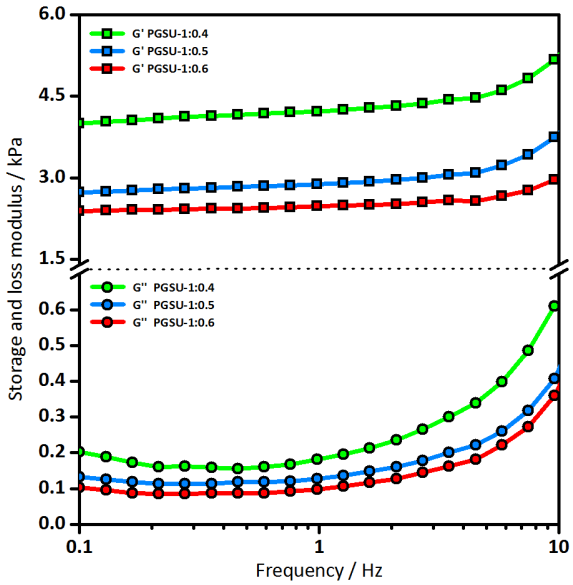

Figure 6. Frequency sweep data for hydrated PGSU scaffolds. The storage modulus (G') and loss modulus (G'') were measured as a function of frequency under oscillatory shear at a strain of 0.1%, in the frequency range of 0.1-10 Hz at 25 °C.

Rheological measurements were performed on hydrated PGSU scaffolds to assess their potential performance in dynamic and wet conditions similar to physiological environments. The storage modulus (G') and loss modulus (G'') as a function of the oscillatory frequency are shown in Figure 6. Briefly, the G' values of the PGSU scaffolds dominated the whole range of frequency and were one to two orders of magnitude higher than corresponding G'' values, suggesting that the bulk response of the hydrated PGSU scaffolds to an applied deformation is mainly elastic, while the G' and G'' values increased slightly with increasing frequency in general. The PGSU-1:0.4 scaffolds presented overall the highest G' and G'' values, due to the

highest scaffold density, lowest porosity and lowest water absorption ability, in comparison to the PGSU-1:0.5 and PGSU-1:0.6 scaffolds which presented similar results.

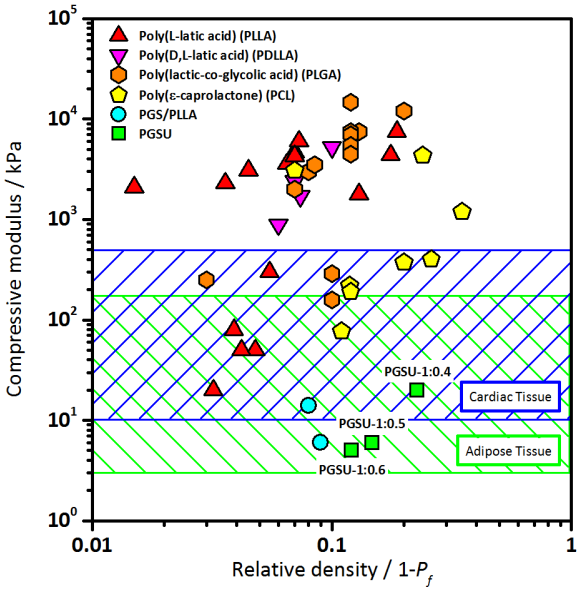

Figure 7. Comparison of the compressive moduli of biopolymer porous scaffolds as a function of relative density between the values of conventional biodegradable polyesters for tissue engineering from the literature (Table S1, Supplementary Content) and the values of PGS-based biopolymers (including this work).[6,8]

Overall, the PGSU scaffolds reported here show excellent mechanical characteristics under quasi-static and cyclic tensile and compressive loads with structurally stable and stretchable properties, suitable to engineer scaffolds for a range of soft tissues, such as human cardiac muscles (Young's modulus: 10-500 kPa)[7,25] or adipose tissue (Young's modulus: 3-180 kPa).[26] As illustrated in Figure 7, at the same relative density, the PGSU scaffolds show a much lower compressive modulus than scaffolds from other porous scaffolds based on conventional synthetic polyesters, such as poly(L-lactic acid), poly(D,L-lactic acid), poly(lactic-co-glycolic acid) and poly(ε-caprolactone). Scaffolds based on these common types of synthetic polyesters are more prone to plastic deformations under external loads, feature stiffer bulk properties and lack of flexibility and strechability. Hence, the elastomeric

PGSU scaffolds mimic the bulk mechanical properties of soft tissues (e.g. adipose and cardiac tissues) more closely. The high flexibility and stretchability of the scaffold constructs indicate that the PGSUs have high potential in soft tissue engineering applications for dynamic environments.

3.4 *In vitro* degradation

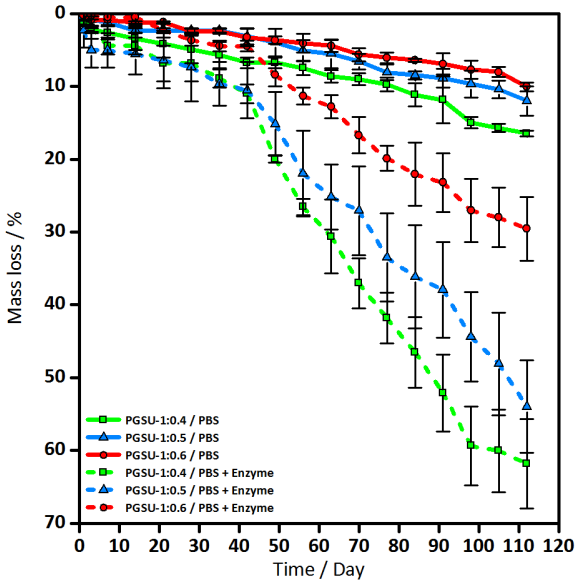

Figure 8. Percentage of mass loss of PGSU scaffolds, incubated with and without the presence of lipase enzyme in PBS for up to 112 days in a shaker incubator at 37 °C and 100 rpm.

The *in vitro* degradation performance of all PGSU scaffolds were analysed in enzyme-free and lipase enzyme-containing PBS solution for up to 112 days, as shown in Figure 8. In the enzyme-free PBS solution the PGSU-1:0.4, PGSU-1:0.5 and PGSU-1:0.6 scaffold specimens obtained degradation degrees of 16%, 12% and 10% in 112 days, while in the enzymatic PBS solution the PGSU specimens exhibited higher degradation degrees of 62%, 54% and 30% in the same time period, respectively. The PGSU scaffolds were characterised with relatively linear degradation kinetics and presented a gradual and visible loss in volume (Figure S3-5,

Supplementary Content), suggesting that the degradation mechanism is based on the surface erosion like PGS.[9] The results also demonstrated that the degradation kinetics of the PGSU scaffolds was dependent on the urethane content in the PGSU specimens, in which slower degradation rates are linked to a higher urethane group number, and *vice versa*.[9] The enzymatically tested PGSU specimens displayed quicker degradation, indicating the catalysed hydrolysis of the ester bonds of the PGS segments due to the lipase enzyme.[27] SEM examination (after 34 days *in vitro* degradation) presented smooth strut surface morphologies for the PGSU scaffolds in enzyme-free PBS solution, while in enzyme-containing PBS solution the specimens showed stronger signs of surface degradation, characterised by rough features (Figure S6-7, Supplementary Content). The PGSU-1:0.6 scaffold specimens presented the slowest degradation, due to their higher degree of crosslinking and more urethane groups, indicating that the degradation rate of PGSU can be tuned and depend on the molar ratio of glycerol to HDI, which is in alignment with previous studies.[9,10]

The *in vitro* degradation tests of the PGSU scaffolds illustrate high potential for designing tissue engineered constructs with long-term stability and tuneable degradation kinetics. Previous *in vitro* degradation studies with large and porous PGS/PLLA scaffolds, containing 73 vol.% PGS and characterised with porosities and pore sizes in the ranges of 91-92% and 109-141 μm, presented mass losses of 11-16% and 54-55% without and with the presence of lipase enzyme in 31 days, respectively.[8] In addition, *in vivo* studies of channelled PGS scaffolds with porosities and pore sizes of ~95% and ~100 μm presented mass losses of up to 80% during the implantation period of 35 days.[28] In comparison, under the same *in vitro* degradation test conditions and period the PGSU scaffolds presented mass losses of 2-6% and 5-10% in the enzyme-free and enzyme-containing PBS solution, respectively, demonstrating significantly reduced degradation rates due to the urethane groups in the chemical structure.[9] Previous *in vivo* studies with PGSU film specimens also demonstrated long-term shape

maintenance and slow degradations rates, in which sample fragmentation was first discovered after 280 days implantation in adult female Lewis rats.[9]

The freeze-dried PGSU scaffolds in this work presented slow degradation kinetics, microstructures with high porosities and interconnected large pores, good hydrophilic characteristics, as well as soft and highly stretchable mechanical properties, demonstrating great potential for long-term soft tissue engineering applications. Compared to other fabrication strategies, the freeze-drying fabrication method is less complex and enables the production of large and porous 3D scaffold constructs with interconnected pores with adjustable dimensions and orientations, capable to fit specific cell types and tissue engineering applications.[6,8,25,29,30] With this respect, PGSU presented in previous studies good *in vitro* cytocompatibility with human mesenchymal stem cells and similar *in vivo* inflammatory reactions compared to poly(lactic-co-glycolic acid) material, which were characterised by mixed lymphohistiocytic infiltrates, however, no adverse reactions or complications were noted during the implantation period.[9] Due to the tunability of PGSU, scaffolds with a broad range of mechanical properties are producible to match those of the native host soft tissues. Soft tissues, e.g. fat, cardiac muscle and blood vessels, are physiologically exposed to large deformations, and exist in a mechanically dynamic environment where the loads can vary spatially and temporally.[31–33] For instance, in the sitting posture, physiological loads induced peak tensile, compressive and shear strains of ~30%, ~45% and ~40% on the anatomical site related fat tissues, as well as tensile, compressive and shear strains of ~75%, ~75% and 91% on the anatomical site related muscle tissues, respectively.[34,35] Conventional synthetic biodegradable polyesters, such as poly(lactic acid), poly(glycolic acid) and their copolymers, although commonly used in tissue engineering, are not stretchable, are subject to plastic deformation, are prone to failure under cyclic deformations, and ultimately cause a mismatch in compliance.[3,25,36] Thus, the

mechanical properties of engineered scaffold constructs are critical for successful surgical implantation.[3,32,37] Ideal engineered soft tissue scaffold should not only be structurally stable to withstand *in vivo* mechanical stresses and deformations, but also feature certain flexibility and stretchability which can provide mechanical stimulation, while providing support to the ingrowing tissue.[3,33] Future work should examine the *in vitro* and *in vivo* tissue growth behaviour of cell-seeded scaffolds, as well as analysing the cell behaviour under mechanical stimulation.

4 Conclusions

Flexible and large 3D porous PGSU scaffolds with different molar ratios of HDI were produced via a freeze-drying process. Results proved that the solvent-based PGSU synthesis with a following freeze-drying and curing process can create stable and highly interconnected open-pore scaffold constructs with no structure collapse. PGSU scaffolds were characterised with non-uniform shapes and smooth pore-wall surfaces, and featured high porosities and pore sizes in the ranges of 77-88% and 55-74 μm, respectively. The PGSU scaffolds exhibited relatively good hydrophilic characteristics, as well as high water absorption abilities. Hydrated PGSU scaffolds obtained a Young's modulus, ultimate tensile strength and elongation at break in the ranges of 29-32 kPa, 12-19 kPa and 50-57%, respectively, and showed no fracture and full recoverability after 75% strain compression. In addition, hydrated PGSU scaffolds presented overall minor hysteresis loss ratio at high strain after cyclic tensile and compression tests, and rheological measurements indicated a primarily elastic bulk response at low strains. PGSU scaffolds were characterised with linear degradation kinetics and obtained *in vitro* degradation rates of 10-16% and 30-62% in 112 days in enzyme-free and enzyme-containing PBS solution, respectively. Overall, the freeze-dried PGSU scaffolds have high potential to be further developed for uses in soft tissue engineering.

Acknowledgements

We thank the Royal Society for financial support (RG120037).

References

[1] I. Levental, P.C. Georges, P.A. Janmey, Soft biological materials and their impact on cell function, Soft Matter, 3 (2007), pp. 299–306.

[2] D.L. Butler, S.A. Goldstein, F. Guilak, Functional tissue engineering: the role of biomechanics, J. Biomech. Eng., 122 (2000), pp. 570–575.

[3] Q. Liu, L. Jiang, R. Shi, L. Zhang, Synthesis, preparation, in vitro degradation, and application of novel degradable bioelastomers - A review, Prog. Polym. Sci., 37 (2012), pp. 715–765.

[4] Y. Wang, G.A. Ameer, B.J. Sheppard, R. Langer, A tough biodegradable elastomer, Nat. Biotechnol., 20 (2002), pp. 602–606.

[5] R. Rai, M. Tallawi, A. Grigore, A.R. Boccaccini, Synthesis, properties and biomedical applications of poly(glycerol sebacate) (PGS): A review, Prog. Polym. Sci., 37 (2012), pp. 1051–1078.

[6] M. Frydrych and B. Chen, Large three-dimensional poly(glycerol sebacate)-based scaffolds – a freeze-drying preparation approach, J. Mater. Chem. B, 1 (2013), pp. 6650–6661.

[7] Q.Z. Chen, A. Bismarck, U. Hansen, S. Junaid, M.Q. Tran, S.E. Harding, N.N. Ali, A.R. Boccaccini, Characterisation of a soft elastomer poly(glycerol sebacate) designed to match the mechanical properties of myocardial tissue, Biomaterials, 29 (2008), pp. 47–57.

[8] M. Frydrych, S. Román, S. MacNeil, B. Chen, Biomimetic poly(glycerol sebacate)/poly(l-lactic acid) blend scaffolds for adipose tissue engineering, Acta Biomater., 18 (2015), pp. 40–49.

[9] M.J.N. Pereira, B. Ouyang, C.A. Sundback, N. Lang, I. Friehs, S. Mureli, I. Pomerantseva, J. McFadden, M.C. Mochel, O. Mwizerwa, P. Del Nido, D. Sarkar, P.T. Masiakos, R. Langer, L.S. Ferreira, J.M. Karp, A highly tunable biocompatible and multifunctional biodegradable elastomer, Adv. Mater., 25 (2013), pp. 1209–1215.

[10] T. Wu, M. Frydrych, K.O. Kelly, B. Chen, Poly(glycerol sebacate urethane) – Cellulose nanocomposites with water-active shape-memory effects, Biomacromolecules, 15 (2014), pp. 2663–2671.

[11] J. Gao, P.M. Crapo, Y. Wang, Macroporous elastomeric scaffolds with extensive micropores for soft tissue engineering, Tissue Eng., 12 (2006), pp. 917–925.

[12] J.S. Chawla, M.M. Amiji, Biodegradable poly(ε-caprolactone) nanoparticles for tumor-targeted delivery of tamoxifen, Int. J. Pharm., 249 (2002), pp. 127–138.

[13] I.H. Jaafar, M.M. Ammar, S.S. Jedlicka, R.A. Pearson, J.P. Coulter, Spectroscopic evaluation, thermal, and thermomechanical characterization of poly(glycerol-sebacate) with variations in curing temperatures and durations, J. Mater. Sci., 45 (2010), pp. 2525–2529.

[14] W. Cai, L. Liu, Shape-memory effect of poly (glycerol-sebacate) elastomer, Mater. Lett., 62 (2008), pp. 2175–2177.

[15] H. Cheng, P.S. Hill, D.J. Siegwart, N. Vacanti, A.K.R. Lytton-Jean, S.W. Cho, A. Ye, R. Langer, D.G. Anderson, A Novel Family of Biodegradable Poly(ester amide) Elastomers, Adv. Mater., 23 (2011), pp. H95–H100.

[16] F.S. Yen, J.L. Hong, Hydrogen-bond interactions between ester and urethane linkages in small model compounds and polyurethanes, Macromolecules, 30 (1997), pp. 7927–7938.

[17] H. Shearer, M.J. Ellis, S.P. Perera, J. B. Chaudhuri, Effects of common sterilization methods on the structure and properties of poly(D,L lactic-co-glycolic acid) scaffolds, Tissue Eng., 12 (2006), pp. 2717–2727.

[18] Z. Pan, J. Ding, Poly(lactide-co-glycolide) porous scaffolds for tissue engineering and regenerative medicine, Interface Focus, 2 (2012), pp. 366–377.

[19] T. Siritientong, T. Srichana, P. Aramwit, The Effect of Sterilization Methods on the Physical Properties of Silk Sericin Scaffolds, AAPS PharmSciTech, 12 (2011), pp. 771–781.

[20] Q.L. Loh, C. Choong, Three-dimensional scaffolds for tissue engineering applications: Role of porosity and pore size, Tissue Eng. Part B, 19 (2013), pp. 485–502.

[21] S.B.G. Blanquer, S.P. Haimi, A.A. Poot, D.W. Grijpma, Effect of pore characteristics on mechanical properties and annulus fibrosus cell seeding and proliferation in designed PTMC tissue engineering scaffolds, Macromol. Symp., 334 (2013), pp. 75–81.

[22] L.J. Gibson, Biomechanics of cellular solids, J. Biomech., 38 (2005), pp. 377–399.

[23] A.J. Kinloch, R.J. Young, Fracture Behaviour of Polymers, Applied Science Publisher, London, 1983.

[24] M. Frydrych, S. Román, N.H. Green, S. MacNeil, B. Chen, Thermoresponsive, stretchable, biodegradable and biocompatible poly(glycerol sebacate)-based polyurethane hydrogels, Polym. Chem., 6 (2015), pp. 7974-7987.

[25] Q.Z. Chen, S.E. Harding, N.N. Ali, A.R. Lyon, A.R. Boccaccini, Biomaterials in cardiac tissue engineering : Ten years of research survey, Mater. Sci. Eng. R, 59 (2008), pp. 1–37.

[26] A. Gefen, E. Haberman, Viscoelastic properties of ovine adipose tissue covering the gluteus muscles, J. Biomech. Eng., 129 (2007), pp. 924–930.

[27] J. Tang, Z. Zhang, Z. Song, L. Chen, X. Hou, K. Yao, Synthesis and characterization of elastic aliphatic polyesters from sebacic acid, glycol and glycerol, Eur. Polym. J., 42 (2006), pp. 3360–3366.

[28] M. Radisic, A. Marsano, R. Maidhof, Y. Wang, G. Vunjak-Novakovic, Cardiac tissue engineering using perfusion bioreactor systems, Nat. Protoc., 3 (2008), pp. 719–738.

[29] H. Zhang, A.I. Cooper, Aligned porous structures by directional freezing, Adv. Mater., 19 (2007), pp. 1529–1533.

[30] J.E. Nichols, J.A. Niles, J. Cortiella, Production and utilization of acellular lung scaffolds in tissue engineering, J. Cell. Biochem., 113 (2012), pp. 2185–2192.

[31] Z. Tong, X. Jia, Biomaterials-based strategies for the engineering of mechanically active soft tissues, MRS Commun., 2 (2012), pp. 31–39.

[32] N. Shoham, A.L. Sasson, F.H. Lin, D. Benayahu, R. Haj-Ali, A. Gefen, The mechanics of hyaluronic acid/adipic acid dihydrazide hydrogel: Towards developing a vessel for delivery of preadipocytes to native tissues, J. Mech. Behav. Biomed. Mater., 28 (2013), pp. 320–331.

[33] S. Mitragotri, J. Lahann, Physical approaches to biomaterial design, Nat. Mater., 8 (2009), pp. 15–23.

[34] E. Linder-Ganz, N. Shabshin, Y. Itzchak, A. Gefen, Assessment of mechanical conditions in sub-dermal tissues during sitting: A combined experimental-MRI and finite element approach, J. Biomech., 40 (2007), pp. 1443–1454.

[35] E. Linder-Ganz, N. Shabshin, Y. Itzchak, Z. Yizhar, I. Siev-Ner, A. Gefen, Strains and stresses in sub-dermal tissues of the buttocks are greater in paraplegics than in healthy during sitting, J. Biomech., 41 (2008), pp. 567–580.

[36] C.J. Bettinger, Synthesis and microfabrication of biomaterials for soft-tissue engineering, Pure Appl. Chem., 81 (2009), pp. 2183–2201.

[37] J. Yang, D. Motlagh, A.R. Webb, G.A. Ameer, Novel biphasic elastomeric scaffold for small-diameter blood vessel tissue engineering, Tissue Eng., 11 (2005), pp. 1876–1886.